A Three-Layer Joint Distributionally Robust Chance-Constrained Framework for Optimal Day-Ahead Scheduling of E-mobility Ecosystem

Mahsa Bagheri Tookanlou^a, S. Ali Pourmousavi Kani^b, Mousa Marzband^{a,c}

^aFaculty of Engineering and Environment, Department of Maths, Physics and Electrical Engineering, Northumbria
University Newcastle, Newcastle upon Tyne NE1 8ST, UK

^b School of Electrical and Electronic Engineering, University of Adelaide, Australia

^cCenter of research excellence in renewable energy and power systems, King Abdulaziz University, Jeddah, Saudi Arabia

Abstract

A high number of electric vehicles (EVs) in the transportation sector necessitates an advanced scheduling framework for e-mobility ecosystem operation to overcome range anxiety and create a viable business model for charging stations (CSs). The framework must account for the stochastic nature of all stakeholders' operations, including EV drivers, CSs, and retailers and their mutual interactions. In this paper, a three-layer joint distributionally robust chance-constrained (DRCC) model is proposed to plan day-ahead grid-to-vehicle (G2V) and vehicle-to-grid (V2G) operations for e-mobility ecosystems. The proposed threelayer joint DRCC framework formulates the interactions of the stochastic behaviour of the stakeholders in an uncertain environment with unknown probability distributions. The proposed stochastic model does not rely on a specific probability distribution for stochastic parameters. An iterative process is proposed to solve the problem using joint DRCC formulation. To achieve computational tractability, the second-order cone programming reformulation is implemented for double-sided and single-sided chance constraints (CCs). Furthermore, the impact of the temporal correlation of uncertain PV generation on CSs operation is considered in the formulation. A simulation study is carried out for an ecosystem of three retailers, nine CSs, and 600 EVs based on real data from San Francisco, USA. The simulation results show the necessity and applicability of such a scheduling framework for the e-mobility ecosystem in an uncertain environment, e.g., by reducing the number of unique EVs that failed to reach their destination from 272 to 61. In addition, the choice of confidence level significantly affects the cost and revenue of the stakeholders as well as the accuracy of the schedules in real-time operation, e.g., for a low-risk case study, the total net cost of EVs increased by 247.3% compared to a high-risk case study. Also, the total net revenue of CSs and retailers decreased by 26.6% and 10.6\%, respectively.

Keywords: Distributionally robust chance-constrained program; E-mobility ecosystem; Grid-to-Vehicle; Vehicle-to-grid; Temporal correlation of uncertain PV generation; Game theory.

Email address: mahsa.tookanlou@northumbria.ac.uk (Mahsa Bagheri Tookanlou)

Nomenclature

Abbreviation

- CCs Chance constraints
- CGU Conventional generation unit
- CSs Charging stations
- DRCC Distributionally robust chance-constrained
- ESS Energy storage system
- EVs Electric vehicles
- G2V Grid-to-vehicle
- RES Renewable generation resources
- SOC State of charge
- V2G Vehicle-to-grid
- VCS Virtual CS

Indices

- e,i,r Index for EVs, CSs, and retailers, respectively
- m, n Index of distribution network nodes
- t Index for hours

Parameters

- Δt Time interval (s)
- $\epsilon_{th}^{\rm EV}/\epsilon_{th}^{\rm CS}/\epsilon_{th}^{\rm re}$ Theoretical risk parameter in each layer
- $\eta_i^{\rm GU}/\eta_i^{\rm CH}$ Efficiency of CGU/chargers at CS i (p.u.)
- η_e^+/η_e^- Efficiency of EV e's battery in G2V/V2G mode (p.u.)
- γ_e Power consumed by EV e per km (kWh/km)
- \mathbb{P} Probability distribution
- $\mathcal{D}_{t,e,i}$ Shortest driving distance between CS i and destination of EV e at time t (km)

- \mathcal{G}_e EV e's driver preference for minimum revenue increase during V2G operation (\$)
- \mathcal{K}_e EV e's driver preference for maximum extra distance to lower the cost compared to minimum route (km)
- $\mathcal{O}_{t,e,i}$ Shortest driving distance between origin of EV e and CS i at time t (km)
- $\overline{\alpha}/\alpha$ Profit margin of the retailer
- $\overline{\rho}^-/\rho^-$ Maximum/Minimum electricity prices offered by CSs for V2G service (\$/kWh)
- $\overline{\rho}^{\rm re}/\rho^{\rm re}$ Maximum/Minimum electricity prices offered by retailers to CSs (\$/kWh)
- $\overline{E}_i^{\text{ESS}}$ Capacity of ESS at CS i (kW)
- $\overline{E}_i^{\rm GU}/\overline{E}_i^{\rm PV}$ Capacity of CGU/PV system at CS i (kW)
- \overline{E}_e Capacity of EV e's battery (kWh)
- \overline{E}_i Capacity of CS i (kW)
- $\overline{E}_i^{\text{CH}}$ Capacity of chargers at CS i (kW)
- $\overline{it}^{CS}/\overline{it}^{re}$ Maximum number of iterations in CS/retailer layer
- $\overline{N}_i^{\text{CH}}$ Maximum number of chargers in CS i
- $\overline{P}_{m,n,t}/\underline{P}_{m,n,t}$ Maximum/Minimum active power flow between node m and n (kW)
- $\overline{Q}_{m,n,t}/\underline{Q}_{m,n,t}$ Maximum/Minimum reactive power flow between node m and n (kVar)
- $\overline{r}_i^{\mathrm{PV}}/\underline{r}_i^{\mathrm{PV}}$ Maximum/Minimum ramping rates of PV generation
- $\overline{SOC}_e/\underline{SOC}_e$ Maximum/Minimum SOC of EV e (p.u.)
- $\overline{SOC}_i^{\mathrm{ESS}}/\underline{SOC}_i^{\mathrm{ESS}}$ Maximum/Minimum SOC of ESS at CS i (p.u.)
- ρ_t^{gas} Natural gas price at time t (\$/ m^3)
- Σ_e Covariance of initial SOC of EV e
- $\Sigma_{t,i}^{PV}$ Covariance of PV generation in CS i at time t
- au_t Covariance of wholesale electricity market prices at time t
- $\Delta V_m/\overline{\Delta V}_m$ Lower/Upper limit of voltage deviation at node m
- ϑ_e EV e's driver preference for minimum cost reduction during G2V operation (\$)
- $\widehat{\mathcal{DO}}_{t,e}$ Driving distance of EV e to closest CS at time t (km)

 $\widehat{\mathcal{O}}_{t,e,i}$ Shortest driving distance between origin of EV e and the nearest CS at t (km)

 $\widetilde{\rho}_t^{\text{WM}}$ Mean wholesale electricity market price at time t (\$/kWh)

 \widetilde{SOC}_{0_e} Mean of initial SOC of EV e

 $\Xi^{EV}/\Xi^{CS}/\Xi^{re}$ Ambiguity set in EV/CS/retailer layer

 $\zeta_{t,e}$ Shortest driving route to reach the destination directly from origin of EV e at time t (km)

a End of day target SOC

b, c, d, f Cost of battery degradation parameters

 $b_{m,n}/g_{m,n}$ Susceptance/conductance of distribution line between node m and n

HV Heat value of fuel on the operation of gas turbine-generator (kWh/m^3)

 it^{CS}/it^{re} Number of iterations in CS/retailer layer

 SOC_e^{end} SOC of EV e at the end of the day (p.u.)

VCS Virtual charging station

e A vector of ones

Sets

 B, E, R, S, T, F_1, F_2 Sets of Nodes, EVs, retailers, CSs, hours, first optional trip time, and second optional trip time, respectively

Variables

 $\beta_{t,i,r}$ Binary variable for retailer r by CS i at time t

 $\Delta \theta_{m,t}$ Voltage angle deviation at node m at time t

 $\Delta V_{m,t}$ Voltage magnitude deviation at node m at time t

 $\Delta \hat{V}_{m,t}$ Voltage magnitude deviation obtained from the lossless power flow solution at node m at time t

 $\Gamma_{t,e,i}/\Pi_{t,e,i}$ Binary variable for CS i for charging/discharging EV e at time t

 $\kappa_{t,r}$ A random variable with zero mean and covariance matrix τ_t for retailer r at time t

 ω_e A random variable with zero mean and covariance matrix Σ_e for EV e

 $\psi_{t,i}$ Binary variable for charging/discharging ESS at CS i

 $\rho_{t,i}^{AG}$ Electricity price sold to the aggregator by CS i at time t (\$/kWh)

 $\rho_{t,i}^+/\rho_{t,i}^-$ Electricity price offered by CS i at time t for charging/discharging EVs (kWh)

 $\theta_{m,t}$ Voltage angle at node m and time t

 $\widehat{A}_{t,e,i}$ Sum of charging and discharging power of EV e in the nearest CS at time t

 $\widehat{
ho}_{t,i}^+/\widehat{
ho}_{t,i}^-$ Electricity price offered by the closest CS to EVs at time t in G2V/V2G mode (kWh)

 $\widetilde{Y}_{t,i}^{\mathrm{PV}}$ Mean local PV generation of CS i at time t (kW)

 $\xi_{t,i}$ A random variable with zero mean and covariance matrix $\Sigma_{t,i}^{PV}$ for CS i at time t

 $A_{t,e,i}$ Sum of charging and discharging power of EV e in CS i at time t

 $P_{m,n,t}/Q_{m,n,t}$ Active/Reactive power flow between node m and n at time t (kW/kVar)

 $P_{t,r}^{\text{WM}}/Q_{t,r}^{\text{WM}}$ Active/Reactive power purchased/provided from/by the wholesale market by retailer r at time t (kW/kVar)

 $SOC_{t,e}$ SOC of EV e at time t (p.u.)

 $V_{m,t}$ Voltage magnitude at node m and time t

 $X_{t,e,i}^+/X_{t,e,i}^-$ Charging/Discharging power of EV e at CS i at time t (kW)

 $Y_{t,i}^{\scriptscriptstyle +}/Y_{t,i}^{\scriptscriptstyle -}$ Charging/Discharging power of ESS of CS i at time t (kW)

 $Y_{t,i}^{\text{GU}}$ Power produced by CGU system of CS i at time t (kW)

 $Y_{t,i,r}^{\mathrm{re}}/Q_{t,i,r}^{\mathrm{re}}$ Active/Reactive power purchased/provided from/by retailer r by CS i at time t (kW/kVar)

 $\rho_{t,r}^{\text{re}}$ Electricity price sold to CSs by retailer r at time t (\$/kWh)

 $\widehat{X}_{t,e,i}^+/\widehat{X}_{t,e,i}^-$ Charging/discharging power of EV e in the nearest CS at time t

 $q_{t,e,i}/I_{t,e,i}$ Additional variables for double-sided CC reformulation in EV layer

 $x_{t,r}/l_{t,r}$ Additional variables for double-sided CC reformulation in retailer layer

 $z_{t,i}/\mu_{t,i}/U_{t,i}/V_{t,i}$ Additional variables for double-sided CCs reformulation in CS layer

1. Introduction

With the increasing adoption of electric vehicles (EVs) in the transportation sector and the rising number of charging stations (CSs) equipped with renewable generation resources (RES), the application of a coordinated vehicle-to-grid (V2G) and grid-to-vehicle (G2V) operation of e-mobility ecosystems has become inevitable under system-wide uncertainties. While day-ahead scheduling can reduce the range anxiety of the EV drivers, the actual driving requirements of the drivers may not be fulfilled by using a deterministic

scheduling framework due to the existence of stochastic parameters; hence leading to ineffective outcomes and drivers' disappointment. In fact, ignoring the impact of the uncertainties in an e-mobility ecosystem may result in significant financial losses for all stakeholders and introduces new challenges for power system operation. Therefore, it indicates the importance of a scheduling framework that accounts for the different sources of uncertainty of the e-mobility ecosystem operation.

The major sources of uncertainty in the future e-mobility ecosystem originate from the EV drivers' behaviour, the unpredictable nature of RES at the CSs and the wholesale electricity market prices [1-4]. To consider these sources of uncertainties in the scheduling problem, various approaches have been proposed in the literature, including robust optimization and scenario-based stochastic programming, which are commonly used to characterise the uncertainties in the transportation sector [5–7]. However, each of these approaches poses certain challenges. An adequate number of scenarios for scenario-based methods must be considered to sufficiently represent the parameters' stochasticity. This is because the performance of the stochastic models depends on the specified scenarios. More often than not, it requires extra computational time; hence intractable in some cases. In robust optimization approaches, the worst-case scenario is considered, which may lead to the most conservative solutions [8]. Also, it is difficult to define a proper probability distribution function for stochastic parameters. To properly address these challenges in stochastic programming, a distributionally robust chance-constrained (DRCC) programming has been developed to consider a moment ambiguity set, which encompasses a family of probability distributions with the firstand second-order moments. Also, DRCC programming allows capturing the temporal correlation of the uncertain parameters by using an ambiguity set with mean and covariance matrix obtained from empirical data. In the following subsections, a comprehensive literature review is presented, followed by a statement listing the contributions of this paper.

1.1. Literature review

In the last decade, numerous research papers investigated EVs' G2V and V2G scheduling problems in an uncertain environment, which can be categorized into (1) scenario-based methods, (2) robust optimization-based methods, and (3) chance-constrained (CC) optimization-based approaches. In the first category, principles of stochastic programming are used for e-mobility ecosystem scheduling. For instance, a scenario-based scheduling scheme for the V2G service was developed in [9]. The availability of plug-in EVs connected to the smart grid was considered an uncertain parameter. The optimal scheduling was obtained by minimizing the overall load variance in the grid. A stochastic optimization model was proposed in [10] to obtain an optimal bidding strategy for the EV aggregator. The uncertainties from the electricity market and EV charging, including the availability and charging pattern of different types of EVs were taken into account in the stochastic optimization model to maximize the profit of the EV aggregator. In [11], a scenario-based risk-constrained stochastic approach was proposed to obtain optimal scheduling of plug-in EVs by aggregators by maximizing their profit in day-ahead and reserve markets. In these studies, a range of parameters, e.g., renewable generation, state of charge (SOC) upon arrival, etc., were treated as stochastic parameters. In

[12], a two-stage scenario-based stochastic program was developed with a rolling horizon for scheduling EVs in G2V operation to meet different grid requirements. The goal was to minimize the difference between EVs' actual and target SOC in a given time period. The arrival and departure times and the initial and target SOC of EV batteries were considered uncertain parameters. A two-stage stochastic model was developed in [13] to optimize the investment decision and operational cost of EVs in the first and second stages, respectively, considering energy consumption and available charging times as the uncertain parameters. A hidden Markov model was used to generate scenarios in that study. In [14], an EV charging scheduling model was presented to minimize the mean waiting time of EVs at CSs with multiple charging points and RES. The EV arrival, the intermittency of the RES, and the electricity prices were considered uncertain parameters and were described by independent Markov processes. In [15], optimal control of a CS with a PV system was investigated based on a finite-horizon Markov decision model under uncertainties of EV drivers and dynamic electricity prices. Then, the total operation cost of the CS was minimized, considering the V2G services and battery degradation. In [16], a two-stage scenario-based stochastic framework was developed for modelling the optimal network of CSs, aiming to find the optimal CS for plug-in hybrid EVs. In that study, stochastic parameters were the battery demand, initial SOC, preferences for charging, and RES generation. In the first stage, the deterministic problem was solved, leading into the second stage, where the final decision was made considering the uncertainties. In [17], a dynamic stochastic optimization problem was formulated to determine optimal EV charging cost considering electricity prices, RES production, and load as stochastic parameters. The authors in [18] proposed a predictive framework by accounting for the uncertainties of EV drivers to achieve cost-effective solutions. In that study, a kernel-based method was used to estimate uncertain parameters during G2V operation.

The second group of studies explored the application of robust optimization for the e-mobility ecosystem operation problem. For example, a multi-objective bi-level stochastic robust optimization problem was proposed in [19] to determine cooperative day-ahead economic-environmental scheduling of the plug-in hybrid EV fleets and a wind farm. In [20], a bi-level robust optimization model was formulated to optimize the design of a CS considering uncertainties in the real-time operation of the CS, including the electricity prices, RES, and the number of EVs. In [5], a robust day-ahead scheduling approach was developed for EV charging in a stochastic environment to deal simultaneously with EV drivers' requirements and distribution network constraints. Several uncertainties were considered, including daily trip distances and arrival and departure times. Furthermore, conservative day-ahead assumptions were considered in the proposed model to address the negative effects of uncertainties. In [21], a robust optimization-based unit commitment model was developed for a system with thermal generators and EV aggregators in a day-ahead V2G scheduling problem. Then, the robust optimization model was reformulated as a deterministic mixed-integer quadratic program using the explicit maximization method, where the single uncertain parameter was the available energy capacity of each EV aggregator. In [22], the robust Stackelberg game was used to investigate the interactions between an aggregator as the leader and several plug-in hybrid EVs as the followers for charging

scheduling under energy demand uncertainty. The application of cooperative and non-cooperative games was investigated to obtain charging schedules and electricity prices for EVs by maximizing the utility of the aggregator. A deterministic optimization problem for optimal EV charging and its robust formulation were compared in [23] under uncertainty of electricity prices. Trade-offs between the optimality of the cost function and robustness of charging scheduling were investigated, and stability of robust charging schedules was obtained concerning uncertain electricity prices. In [24], robust scheduling of EV aggregators' operation was investigated under electricity price uncertainty to maximize their profit. In [25], a Stackelberg game was proposed for the EV aggregator (as the leader) and EVs (as followers) to determine optimal day-ahead charging and frequency reserve scheduling aiming to balance the benefits of the players in the game. A robust optimization approach investigated EVs' optimal schedules under uncertain frequency regulation signals.

Several studies in this field have investigated the application of CC optimization. For instance, to consider the stochastic nature of the EV drivers in [26], a CC optimization problem of EV aggregators and the distribution system operator was developed as a mixed-integer quadratic program. The goal was to reduce the congestion in the distribution network with many EVs. In [27], the CC programming was used to develop a day-ahead scheduling strategy for an EV battery swapping station, where EVs, the number of swapped batteries and PV generation were the source of uncertainties, described by a probabilistic sequence. In [28], a two-stage program for the energy management system of the distribution networks was presented with EVs and RES. In the first stage, a CC model was solved to obtain the optimal operation of CSs and battery swapping stations under uncertainties of RES generation. In the second stage, the EV charging power was determined to meet the EV's charging demand following the optimal operation of CSs.

Based on the comprehensive literature review presented above, we identified four gaps in knowledge concerning EV scheduling in an e-mobility ecosystem as follows:

- **G1:** The interactions between stochastic parameters originated from different stakeholders in an emobility ecosystem were ignored because every stakeholder's operation was optimized individually. In other words, the mutual impacts of the stochastic behaviour of the stakeholders in an uncertain environment have not been investigated in the existing studies. We tried to fill this gap by C1;
- G2: Specific probability distribution functions were assumed for modelling of stochastic parameters, which are an estimation of the true underlying stochastic model [29]. We addressed this issue by defining an ambiguity set and solved the problem using DRCC reformulation in C1;
- **G3:** The proposed CC models in the literature treated the lower and upper bounds as two single-sided CCs, which may lead to over- or under-estimation of the parameters; hence constraints violation in reality. This shortcoming is addressed by C2;
- **G4:** The impact of temporal correlation of PV generation uncertainty on CSs operation has not been investigated in a CC formulation for an e-mobility ecosystem, which is covered in our paper by C3.

1.2. Main Contributions

In this paper, a three-layer joint DRCC framework is proposed to schedule V2G and G2V operation in the day ahead for an e-mobility ecosystem, including EVs, CSs, and retailers in an uncertain environment with unknown probability distributions. In an attempt to facilitate the investigation of an uncertain e-mobility ecosystem, the interactions between the stochastic nature of the three stakeholders are considered in the proposed model. A family of probability distributions with the same mean and covariance matrix called a moment-based ambiguity set is defined to solve a stochastic program without relying on a specific distribution function. An exact second-order cone programming reformulation of joint DRCC day-ahead scheduling framework is developed, which ensures that violation of both upper and lower limits of a constraint remains small for the worst-case probability under the ambiguity set. Furthermore, the temporal correlation of the PV system generation in each time interval is considered in the joint DRCC model.

The main contributions of this paper addressing the gaps mentioned in Section 1.1 are:

- C1: Formulating the interactions of the stochastic behaviour of stakeholders in an e-mobility ecosystem: The proposed three-layer joint DRCC framework allows scheduling V2G and G2V operations in the day ahead for an e-mobility ecosystem, including EVs, CSs, and retailers in an uncertain environment with unknown probability distributions. Therefore, the interactions between the stochastic parameters of the three stakeholders are captured in the proposed framework.
- C2: An exact reformulation of DRCC day-ahead scheduling for e-mobility ecosystem: An exact second-order cone programming reformulation of the joint DRCC is developed in this application, which ensures that violation of both upper and lower limits of a constraint remains small for the worst-case probability under the ambiguity set. To the best of our knowledge, this has not been done in this field.
- C3: Temporal correlation of PV generation: The temporal correlation of the PV system generation is considered in the joint DRCC model, which allows us to see its impact on the operation of the entire ecosystem.

The rest of this paper is structured as follows: Section 2 presents the problem definition and describes the stochastic G2V and V2G framework, including the three stakeholders. It is followed by the proposed three-layer joint DRCC formulation in Section 3. In Section 4, an ecosystem based on 600 EVs, nine CSs, and three retailers is devised for simulation study and the results are discussed. The concluding remarks are presented in Section 5. In Appendix A, reformulation of the single-sided and double-sided CCs in EV, CS, and Retailer layers is demonstrated and explained.

2. Problem Definition

This paper offers a three-layer joint DRCC scheduling framework, where DRCC model is developed for each stakeholder; hence, three layers. In each layer, the uncertainty of each player is modelled using a moment-based ambiguity set consisting of a family of probability distributions for each uncertain parameter. The ambiguity set is formed using the first- and second-order moments, i.e, mean and covariance, of available historical data.

In the proposed ecosystem, illustrated in Fig. 1, we consider R number of retailers, indexed by $r \in$ $\{1,2,\ldots,R\}$. Retailers purchase electricity in the wholesale market to sell it to CSs. Therefore, wholesale electricity price at time t is retailers' major source of uncertainty. There are S number of CSs in the ecosystem, indexed by $i \in \{1, 2, ..., S\}$, that are physically located in the scheduling area. They operate at the distribution network level and provide V2G and G2V services to EVs. Without loss of generality, it is assumed that each CS possesses a small gas turbine/diesel generator as a conventional generation unit (CGU), PV, and energy storage system (ESS) to supply electricity to EVs during G2V operation. Also, CSs purchase electricity from EVs and sell it in the wholesale electricity market through aggregators [30]. Therefore, PV generation is the main source of uncertainty in the CS layer. EVs, in turn, affect the operation/profit of CSs and retailers by their preferences, day-ahead travel plans, initial SOC, time of availability, etc., which is reflected in their G2V/V2G schedules. During a typical day, EVs can have two kinds of trips: mandatory and optional. An EV can have multiple mandatory and optional trips during a day [30]. While a mandatory trip must be fulfilled at any cost, the optional trips will be selected only if the prices are right for G2V and/or V2G services. In other words, an optional trip, as opposed to a mandatory trip, allows EV drivers to take advantage of cheap G2V or expensive V2G services outside of the mandatory trip time frame, thus reducing their overall cost. In our previous paper [30], we have shown that the optional trips can improve the practical aspects of the EV scheduling problem, facilitate higher participation in the G2V and V2G services, and enhance convenience and flexibility in EV scheduling. It is assumed that EV drivers are daily commuters who leave for work in the morning (first mandatory trip) and return home in the evening (second mandatory trip). Between the two mandatory trips (for example, during lunchtime), EV drivers have a chance for a V2G or G2V trip (optional), so they can declare it in their daily plan to the scheduling entity. In this paper, it is assumed that each EV can have two optional trips between mandatory trips. In this approach, each EV driver is allowed to nominate one or two optional trips during a day to reduce its cost. Finally, EVs with a known location and initial SOC, which is the source of uncertainty in the EV layer, seek G2V and V2G plans for their combined mandatory and optional trips to minimise their overall cost while fulfilling their preferences. A day before the scheduling day, EV drivers send their plan to the scheduling centre, e.g., a cloud-based scheduling system, where the scheduling problem is solved for the day-ahead operation of the ecosystem. The optimal schedules will then be communicated back to the EV owners. Please note that most EV drivers are commuters; hence, there is no day-to-day change in their travel plan. Therefore, they do not need to send a new travel plan daily. The driving routes between CS i and the origin of EV e in each trip are known, and only one of the CSs might be selected for EV e. Thus, two binary variables are assigned to each CS for the G2V and V2G operation of the EV e in each interval. The virtual CS (VCS) is considered for the case in which the most economical decision for EV e is not to be charged nor discharged in a trip. Thus by selecting a VCS, EV e reaches the destination from its origin without charging or discharging, while the EV's preferences and constraints are satisfied. The only difference between a mandatory and optional trip is that the driving route of a VCS is zero in an optional trip. Please see [30] for further details about our modelling approach.

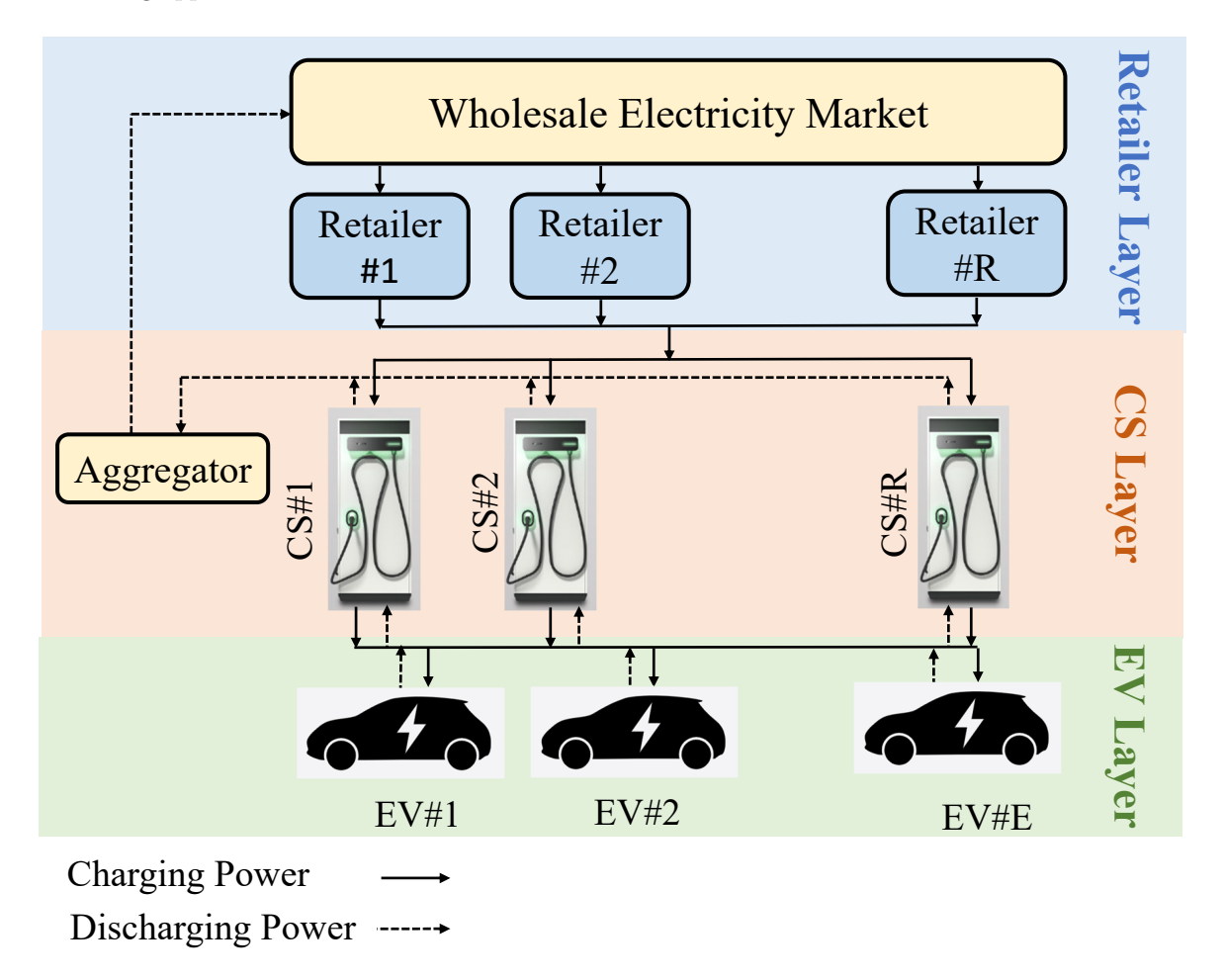


Figure 1: Schematic diagram of the e-mobility ecosystem.

3. The Proposed Framework

In this section, the day-ahead joint DRCC V2G and G2V scheduling framework, which includes several uncertain and deterministic constraints, is presented for each layer based on the deterministic model formulated by the authors in [30]. A general formulation looks like Eq. 1, which finds minimizers x to $f: \mathbb{R}^n \longrightarrow \mathbb{R}$ as the objective function of a CC program subject to a set of deterministic constraints (D) and stochastic constraints $(H(x,\lambda) \leq 0, H: \mathbb{R}^n \times \Lambda \longrightarrow \mathbb{R}^m)$. H is needed to satisfy any probability distribution (\mathbb{P}) from the ambiguity set (Ξ) at a given confidence level $(1-\epsilon) \in (0,1)$.

$$c^* = \min \left\{ f(x) : x \in D, \inf_{\mathbb{P} \in \Xi} \mathbb{P} \left[\lambda \in \Lambda : \{ H(x, \lambda) \le 0 \} \right] \ge 1 - \epsilon \right\}. \tag{1}$$

In the joint DRCC, the uncertain parameter is modelled by $\mu + \omega$, where μ is the mean of the uncertain parameter and ω is a random variable with zero mean and covariance matrix Σ . The ambiguity set is defined by

$$\Xi = \{ \mathbb{P} \in \Xi(\mathbb{R}^{\nu}) : \mathbb{E}_{\mathbb{P}}[\omega], E_{\mathbb{P}}[\omega\omega^{T}] = \Sigma \}.$$
(2)

In the literature, moment-based and metric-based ambiguity sets are widely used. A moment-based ambiguity set includes all probability distributions with identical mean and covariance. In the metric-based ambiguity set, however, a ball is defined in the space of distribution functions. The centre of the ball is the empirical distribution, and the ball is built around the centre using a probability distance function such as ϕ -divergence or Wasserstein metrics [31, 32]. Although the metric-based ambiguity set leads to a relatively stronger performance, the moment-based ambiguity set is proven to be more tractable [32]. For instance, the authors in [32] showed that a distributionally robust model constructed based on the Wasserstein metric is more computationally expensive and is not cost-effective compared to the moment-based ambiguity set. Therefore, we preferred the moment-based ambiguity set in our study, considering the size of our optimization problem involving three layers of sequential games. The DRCC models for EV, CS, and Retailer layers are presented in Section 3.1, 3.2, and 3.3, respectively. The exact reformulation of the single-sided and double-sided CCs are presented in Theorems 1 and 2 in [33]. The reformulation of our optimization problem is described in Appendix A.

The proposed three-layer scheduling framework is solved by an iterative approach shown in Fig. 2. The retailers estimate wholesale electricity prices using historical data in the first iteration. Then, the prices are passed on to the CS layer. In this iteration, the prices are only inflated to consider the CSs' profit margin. Then, the CSs' will determine their prices accordingly (both G2V and V2G) and send them to the EV layer, where the first DRCC problem will be solved in the first iteration. The DRCC problem will be solved in the EV layer under the uncertainty of the EV's initial SOC. The results are the EVs' charging and discharging power and selected CSs for every EV during each trip. The decision to select a CS is based on rationality (i.e., cost reduction) and comfort (i.e., drivers' preferences). Upon receiving the results from the EV layer, the CS layer solves the DRCC problem to obtain the new G2V and V2G prices according to the reaction of EVs. This inner loop between CS and EV layers, as shown in Fig. 2, will continue until the convergence criterion of the DRCC problem in the CS layer under PV generation uncertainty is satisfied. Afterwards, selected retailers and the amount of purchasing power from each retailer will be communicated to the retailer layer. Then, the DRCC problem in the retailer layer is solved considering the uncertainty of the wholesale electricity prices. In the retailer layer, new electricity prices will be determined according to the collective reactions of the CSs and EVs to the original prices. The second iteration of the outer loop, as shown in Fig. 2, starts with the new retailers' prices. This iterative process will be terminated once the difference between the relevant objective functions in the last two iterations for inner and outer loops is less than or equal to 0.001.

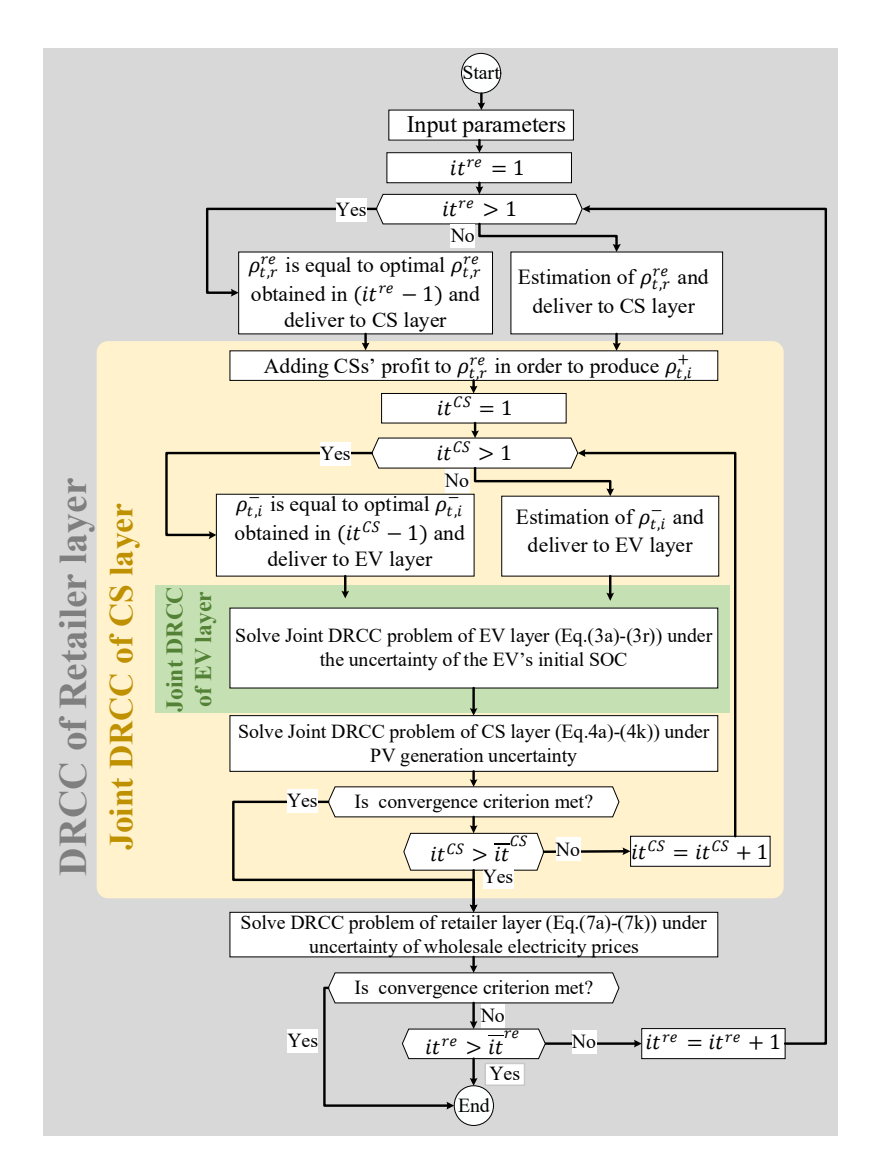


Figure 2: Flowchart of the three-layer joint DRCC problem

3.1. Joint DRCC Model in the EV Layer

The proposed DRCC model in the EV layer minimises the net cost of EV operation during V2G and G2V services. The proposed problem is constrained by a set of distributionally robust CC in Eqs. (3d), (3e), (3j), and (3k). Equations (3b) and (3c) indicate the sum of the charging and discharging power of EV e in CS i and the nearest CS, respectively, at time t. Equation (3d) signifies that under the worst distribution in ambiguity set for the EV layer (Ξ^{EV}), the probability of maintaining the SOC level of EV e within a lower and upper bound at all times must be greater than or equal to a given confidence level. The DRCC in Eq. (3e) points to fulfil target SOC of EV e at the end of the day within a permissible range (i.e., between the target and maximum SOC). Admissible charging and discharging capacity of the chargers at CS i are imposed by Eqs. (3f) and (3g). To select one CS for either G2V and V2G services by EV e at time t, sum of the binary variables of CSs must be less than or equal to one, as in by Eq. (3h). Furthermore,

Eq. (3i) guarantees that the number of used chargers at a CS for charging and discharging does not exceed the number of existing chargers. The DRCC in Eqs. (3j) and (3k) impose driver's cost/revenue threshold limitations for selecting an alternative route instead of the shortest route during V2G and G2V operation. The driver's route preferences for charging/discharging EV e at time t in an alternative CS other than the nearest CS are ensured by Eqs. (3l) and (3m). The zero power of charging and discharging at a VCS must be set to zero, which is achieved by Eqs. (3n) and (3o). Equation (3p) sets the driving route allocated to VCS for the mandatory trip, which is equal to the shortest route to reach the destination directly from the origin of EV e. The driving route distance between EV and VCS in the first and second optional trips are set to zero by Eqs. (3q) and (3r).

$$\min_{\substack{X_{t,e,i}^+, X_{t,e,i}^-, \\ \Gamma_{t,e,i}, \Pi_{t,e,i}}} \sup_{\mathbb{P} \in \Xi^{EV}} \mathbb{E}_{\mathbb{P}} \left[\sum_{t=1}^T \sum_{e=1}^E X_{t,e,i}^+ \cdot \rho_{t,i}^+ \right. \\
\left. + \left(b \cdot \left(SOC_{t,e} - a \cdot (\Gamma_{t,e,i} + \Pi_{t,e,i}) \right)^2 \right. \\
\left. + c.X_{t,e,i}^+ - d.X_{t,e,i}^- + f.X_{t,e,i}^{-2} \right) \right. \\
\left. - X_{t,e,i}^- \cdot \rho_{t,i}^- \right] \qquad \forall i \in S, \tag{3a}$$

s.t.

$$A_{t,e,i} = \frac{\eta_e^+ \cdot \sum_{t=1}^t X_{t,e,i}^+ \cdot \Delta t}{\overline{E}_c} - \frac{\sum_{t=1}^t X_{t,e,i}^- \Delta t}{\eta^- \overline{E}_c},$$
(3b)

$$\widehat{A}_{t,e,i} = \frac{\sum_{t=1}^{t} \eta_e^+ . \widehat{X}_{t,e,i}^+ \Delta t}{\overline{E}_e} - \frac{\sum_{t=1}^{t} \widehat{X}_{t,e,i}^- \Delta t}{\overline{E}_{e,i} \eta_e^-}, \tag{3c}$$

$$\inf_{\mathbb{P} \in \Xi^{EV}} \mathbb{P} \left[\underline{SOC}_{e} \leq \overline{SOC}_{0_{e}} - e^{T} \omega_{e} + A_{t,e,i} \right] \\
- \sum_{t=1}^{t} \frac{\zeta_{t,e} \cdot \gamma_{e}}{\overline{E}_{e}} \cdot (1 - \Gamma_{t,e,i} - \Pi_{t,e,i}) - \frac{\mathcal{O}_{t,e,i} \cdot \gamma_{e}}{\overline{E}_{e}} \cdot (\Gamma_{t,e,i} + \Pi_{t,e,i}) \leq \overline{SOC}_{e} \right] \geq 1 - \epsilon_{th}^{EV} \tag{3d}$$

$$\forall t \in T, \forall e \in E, \forall i \in S,$$

$$\inf_{\mathbb{P}\in\Xi^{EV}} \mathbb{P} \left[SOC_e^{\text{end}} \leq \widetilde{SOC}_{0_e} - e^T \omega_e + A_{T,e,i} \right] \\
- \sum_{t=1}^{T} \frac{\zeta_{t,e} \cdot \gamma_e}{\overline{E}_e} \left(1 - \Gamma_{t,e,i} - \Pi_{t,e,i} \right) - \frac{\mathcal{O}_{T,e,i} \cdot \gamma_e}{\overline{E}_e} . \\
\left(\Gamma_{T,e,i} + \Pi_{T,e,i} \right) \leq \overline{SOC}_e \right] \geq 1 - \epsilon_{th}^{EV}$$
(3e)

 $\forall t \in T, \forall e \in E, \forall i \in S.$

$$0 \le X_{t,e,i}^+ \le \overline{E}_i^{\mathrm{CH}}.\Gamma_{t,e,i} \quad \forall t \in T, \forall e \in E, \forall i \in S, \tag{3f}$$

$$0 \le X_{t,e,i}^{-} \le \overline{E}_{i}^{\mathrm{CH}}.\Pi_{t,e,i} \quad \forall t \in T, \forall e \in E, \forall i \in S,$$

$$(3g)$$

$$\sum_{i=1}^{S} (\Pi_{t,e,i} + \Gamma_{t,e,i}) \le 1 \quad \forall t \in T, \forall e \in E,$$
(3h)

$$\sum_{e \in E} (\Gamma_{t,e,i} + \Pi_{t,e,i}) \le \overline{N}_i^{CH} \quad \forall t \in T, \forall i \in S,$$
(3i)

$$\inf_{\mathbb{P}\in\Xi^{EV}} \mathbb{P}\left[\rho_{t,i}^{+}.X_{t,e,i}^{+} \leq \vartheta_{e}.\Gamma_{t,e,i} + \widehat{\rho}_{t,i}^{+}.\overline{E}_{e}.\Gamma_{t,e,i}\right] \\
\cdot \left(\widetilde{SOC}_{e} - e^{T}\omega_{e} + \widehat{A}_{t,e,i} - \frac{\widehat{\mathcal{O}}_{t,e,i}.\gamma_{e}}{\overline{E}_{e}}\right) \\
- \widehat{\rho}_{t,i}^{+}.\overline{E}_{e}.(1 - \Gamma_{t,e,i}).\sum_{t=1}^{t} \frac{\zeta_{t,e}.\gamma_{e}}{\overline{E}_{e}} \ge 1 - \epsilon_{th}^{EV}$$
(3j)

 $\forall t \in T, \forall e \in E, \forall i \in S,$

$$\inf_{\mathbb{P}\in\Xi^{EV}} \mathbb{P}\left[\rho_{t,i}^{-}.X_{t,e,i}^{-} \geq \mathcal{G}_{e}.\Pi_{t,e,i} + \widehat{\rho_{t,i}}.\overline{E}_{e}.\Pi_{t,e,i}\right] \\
\cdot \left(\widetilde{SOC}_{e} - e^{T}\omega_{e} + \widehat{A}_{t,e,i} - \frac{\widehat{\mathcal{O}}_{t,e,i}.\gamma_{e}}{\overline{E}_{e}}\right) \\
- \widehat{\rho_{t,i}}.\overline{E}_{e}.(1 - \Pi_{t,e,i}).\sum_{t=1}^{t} \frac{\zeta_{t,e}.\gamma_{e}}{\overline{E}_{e}}\right] \geq 1 - \epsilon_{th}^{EV}$$
(3k)

 $\forall t \in T, \forall e \in E, \forall i \in S,$

$$\Gamma_{t,e,i}.(\mathcal{O}_{t,e,i} + \mathcal{D}_{t,e,i}) \le (\widehat{\mathcal{DO}}_{t,e} + \mathcal{K}_e).\Gamma_{t,e,i}$$
(31)

 $\forall t \in T, \forall e \in E, \forall i \in S,$

$$\Pi_{t,e,i} \cdot (\mathcal{O}_{t,e,i} + \mathcal{D}_{t,e,i}) \le (\widehat{\mathcal{D}\mathcal{O}}_{t,e} + \mathcal{K}_e) \cdot \Pi_{t,e,i}$$
(3m)

 $\forall t \in T, \forall e \in E, \forall i \in S,$

$$X_{t,e,i}^+ = 0 \qquad \forall t \in T, \forall e \in E, \forall i = VCS,$$
 (3n)

$$X_{t,e,i}^- = 0 \qquad \forall t \in T, \forall e \in E, \forall i = VCS,$$
 (30)

$$\mathcal{O}_{t,e,i} + \mathcal{D}_{t,e,i} = \zeta_{t,e} \,\forall t \in (T - F_1 - F_2), \,\forall e \in E, \,\forall i = VCS, \tag{3p}$$

$$\mathcal{O}_{t,e,i} + \mathcal{D}_{t,e,i} = 0 \quad \forall t \in F_1, \forall e \in E, \forall i = VCS, \tag{3q}$$

$$\mathcal{O}_{t,e,i} + \mathcal{D}_{t,e,i} = 0 \quad \forall t \in F_2, \forall e \in E, \forall i = VCS.$$
(3r)

3.2. Joint DRCC Model in the CS Layer

The DRCC model in the CS layer is presented in this section as a maximization of the net revenue of all CSs. The sum of the CSs' revenue is the objective function of the DRCC problem in the CS layer, as in Eq. (4). The revenue of CS i is obtained by selling electricity to EV e and the aggregator during G2V and V2G operation, respectively. The cost of CS i consists of the operational cost of CGU, the cost of electricity purchased from retailer r and EV e in G2V and V2G services, respectively.

$$\max_{\substack{Y_{t,i,r}^{re}, Y_{t,i}^{GU}, \widetilde{Y}_{t,i}^{PV} \\ Y_{t,i}^{t}, Y_{t,i}^{-}, \rho_{t,i}^{-}, \\ \beta_{t,i,r}, \psi_{t,i}}} \sup_{\mathbb{P} \in \Xi^{CS}} \mathbb{E}_{\mathbb{P}} \left[\sum_{t=1}^{T} \sum_{i=1}^{S} \sum_{e \in E} (X_{t,e,i}^{+}, \rho_{t,i}^{+} \\ + X_{t,e,i}^{-}, \rho_{t,i}^{AG}) \right] \\
-Y_{t,i,r}^{re}, \rho_{t,r}^{re} - \sum_{e \in E} X_{t,e,i}^{-}, \rho_{t,i}^{-}$$
(4a)

$$-Y_{t,i,r}^{\text{IC}} \cdot \rho_{t,r}^{\text{IC}} - \sum_{e \in E} X_{t,e,i} \cdot \rho_{t,i}$$
$$-\frac{Y_{t,i}^{\text{GU}} \cdot \rho_{t}^{\text{gas}}}{\eta_{i}^{\text{GU}} \cdot HV} \bigg] \qquad \forall r \in R,$$

s.t.

$$\inf_{\mathbb{P} \in \Xi^{CS}} \mathbb{P} \left[\widetilde{Y}_{t,i}^{\text{PV}} - \mathbf{1}^{\text{T}} \xi_{t,i} + Y_{t,i}^{\text{GU}} + Y_{t,i,r}^{\text{re}} + Y_{t,i}^{-} + \sum_{e \in E} X_{t,e,i}^{-} + \sum_{e \in E} X_{t,e,i}^{-} + \varepsilon \ge \frac{\sum_{e \in E} X_{t,e,i}^{-}}{\eta_{i}^{\text{CH}}} + \frac{\sum_{e \in E} X_{t,e,i}^{+}}{\eta_{i}^{\text{CH}}} + Y_{t,i}^{+} \right] \ge 1 - \epsilon_{th}^{CS}$$
(4b)

 $\forall t \in T, \forall i \in S, \forall r \in R,$

$$0 \le Y_{t,i}^{\mathrm{GU}} \le \overline{E}_{i}^{\mathrm{GU}} \quad \forall t \in T, \forall i \in S, \tag{4c}$$

$$\inf_{\mathbb{P} \in \Xi^{CS}} \mathbb{P} \left[0 \le \widetilde{Y}_{t,i}^{PV} - \mathbf{1}^{T} \xi_{t,i} \le \overline{E}_{i}^{PV} \right] \ge 1 - \epsilon_{th}^{CS} \quad \forall t \in T, \forall i \in S,$$
(4d)

$$\inf_{\mathbb{P} \in \Xi^{\text{CS}}} \mathbb{P} \left[\underline{r}_{i}^{\text{PV}} \leq \frac{\widetilde{Y}_{t,i}^{\text{PV}} - \widetilde{Y}_{t-1,i}^{\text{PV}} - \widehat{\xi}_{t,i}}{\Delta t} \leq \overline{r}_{i}^{\text{PV}} \right] \geq 1 - \epsilon_{th}^{\text{CS}}, \tag{4e}$$

$$0 \le Y_{t,i,r}^{\text{re}} \le \overline{E}_i.\beta_{t,i,r} \quad \forall t \in T, \forall i \in S, \forall r \in R, \tag{4f}$$

$$\sum_{r=1}^{R} \beta_{t,i,r} \le 1 \quad \forall t \in T, \forall i \in S, \tag{4g}$$

$$0 \le Y_{t,i}^+ \le \overline{E}_i^{\text{ESS}}.\psi_{t,i} \quad \forall t \in T, \forall i \in S, \tag{4h}$$

$$0 \le Y_{t,i}^{-} \le \overline{E}_{i}^{\mathrm{ESS}}.(1 - \psi_{t,i}) \quad \forall t \in T, \forall i \in S,$$

$$\tag{4i}$$

$$\underline{SOC_{i}^{\mathrm{ESS}}} \leq \frac{\sum_{t=2}^{t} (Y_{t,i}^{+} - Y_{t,i}^{-}) \cdot \Delta t}{\overline{E_{i}^{ESS}}} \leq \overline{SOC_{i}^{\mathrm{ESS}}} \quad \forall t \in T, \forall i \in S,$$

$$(4j)$$

$$\underline{\rho}^- \le \rho_{t,i}^- \le \overline{\rho}^- \quad \forall t \in T, \forall i \in S. \tag{4k}$$

There exists a set of DRCCs as in Eqs. (4b), (4d), (4e) in this layer. The probability of maintaining the power balance between supply and demand at CS i under the worst distribution in the ambiguity set (Ξ^{CS}) is imposed by Eq. (4b). The lower and upper capacity limits of CGU are enforced by Eq. (4c). The DRCC to fulfil the lower and upper capacity limits of PV generation at CS i is given in Eq. (4d). Equation (4e) represents the temporal correlation of renewable energy production. For this constraint, the uncertainty parameter contains both $\xi_{t,i}$ and $\xi_{t-1,i}$ as:

$$\widehat{\xi}_{t,i} = \begin{bmatrix} \xi_{t,i} \\ \xi_{t-1,i} \end{bmatrix}. \tag{5}$$

In order to consider the effect of temporal correlation on Eq. (4e), a covariance matrix is defined as [29]:

$$\widehat{\Sigma}_{t,i}^{\text{PV}} = \begin{bmatrix} \Sigma_{t,i}^{\text{PV}} & \Upsilon_{(t,t-1),i}^{\text{PV}} \\ \Upsilon_{(t,t-1),i}^{\text{PV}} & \Sigma_{t-1,i}^{\text{PV}} \end{bmatrix}.$$

$$(6)$$

The electricity purchased from retailer r is constrained by Eq. (4f). Equation (4g) guarantees that only one retailer is selected by CS i at time t. The limitation of charging and discharging power of ESS at CS i are enforced by Eqs. (4h) and (4i). The SOC of ESS must be within a permissible range, which is enforced by Eq. (4j). Equation (4k) ensures that the electricity prices in V2G services are limited by its minimum and maximum bounds for the DRCC problem in the CS layer.

3.3. DRCC Model in the Retailer Layer

The DRCC model in the Retailer layer is presented in this section as a maximization of the net revenue of all retailers. It consists of the difference between revenue obtained by selling electricity to CS i, and the cost of electricity purchased from the wholesale electricity market, as given in Eq. (7). The wholesale electricity prices are the stochastic parameter in this layer.

$$\max_{\widetilde{\rho}_{t,r}^{re}} \sup_{\mathbb{P} \in \Xi^{CS}} \mathbb{E}_{\mathbb{P}} \left[\sum_{t=1}^{T} \sum_{r=1}^{R} \sum_{i \in S} Y_{t,i,r}^{re} . \rho_{t,r}^{re} - P_{t,r}^{WM} . (\widetilde{\rho}_{t}^{WM} - \mathbf{1}^{T} \kappa_{t}) \right] \quad \forall i \in S,$$
(7a)

s.t.

$$P_{t,r}^{\text{WM}} = \sum_{i \in S} Y_{t,i,r}^{re},\tag{7b}$$

$$Q_{t,r}^{\text{WM}} = \sum_{i \in S} Q_{t,i,r}^{re},\tag{7c}$$

$$P_{m,n,t} = g_{m,n} \cdot (1 + \Delta \hat{V}_{m,t}) \cdot (\Delta V_{m,t} - \Delta V_{n,t})$$
(7d)

$$-b_{m,n}.(\theta_{m,t}-\theta_{n,t}) \quad \forall m,n \in B, \forall t \in T,$$

$$Q_{m,n,t} = -b_{m,n} \cdot (1 + \Delta \hat{V}_{m,t}) \cdot (\Delta V_{m,t} - \Delta V_{n,t})$$
(7e)

$$-g_{m,n}.(\theta_{m,t}-\theta_{n,t}) \quad \forall m,n \in B, \forall t \in T,$$

$$V_{m,t} = 1 + \Delta V_{m,t} \quad \forall m \in B, \forall t \in T, \tag{7f}$$

$$\theta_{m,t} = 0 + \Delta \theta_{m,t} \quad \forall m \in B, \forall t \in T, \tag{7g}$$

$$\underline{\Delta V}_m \le \Delta V_{m,t} \le \overline{\Delta V}_m \quad \forall m \in B, \tag{7h}$$

$$\underline{P}_{m,n} \le P_{m,n,t} \le \overline{P}_{m,n} \quad \forall m, n \in B, \forall t \in T,$$
(7i)

$$Q_{m,n} \le Q_{m,n,t} \le \overline{Q}_{m,n} \quad \forall m, n \in B, \forall t \in T, \tag{7j}$$

$$\inf_{\mathbb{P} \in \Xi^{re}} \mathbb{P} \left[\underline{\alpha}_{t} \times \widetilde{\rho}_{t}^{\text{WM}} - \mathbf{1}^{T} \kappa_{t} \leq \rho_{t,r}^{\text{re}} \leq \overline{\alpha}_{t} \times \widetilde{\rho}_{t}^{\text{WM}} - \mathbf{1}^{T} \kappa_{t} \right]$$

$$\geq 1 - \epsilon_{th}^{re}.$$
(7k)

Equations (7b) and (7c) enforce the active and reactive power balance at time t, respectively. Thus, the electricity purchased from the wholesale electricity market through retailer r must be equal to sum of the

electricity purchased by CSs from retailer r for active and reactive power at time t. Equations (7d) and (7e) satisfy real and reactive power flows in the network considering voltage magnitude and angle deviations determined by Eqs. (7f) and (7g). Equation (7h) fulfils the minimum and maximum nodal voltage limits. Equations (7i) and (7j) guarantee that active and reactive power is maintained within a standard range. The probability of maintaining the electricity prices offered by retailers between maximum and minimum bounds under the worst distribution ambiguity set in the Retailer layer (Ξ^{re}) is imposed by Eq. (7k).

4. Simulation Results

We implemented the proposed day-ahead DRCC scheduling framework in a simulation study with three retailers, nine CSs, and 600 EVs in a small area of San Francisco, USA, using the IEEE 37-node distribution test system to assess its performance under different conditions. 30 bidirectional 50 kW DC chargers are assumed to be available at each CS. Every CS is equipped with a 65 kW CGU, a PV system (randomly selected from {16, 19.2, 24, 27.2, 32} kW set) and a one-hour ESS (randomly selected from {45, 50, 65, 70, 85} kW set). The mean value of the initial SOC of EVs is assumed to be between 10% and 95%, and the covariance of the initial SOC of each EV is equal to 5%. It is assumed that EV drivers are daily commuters who leave for work in the morning (first mandatory trip) and return home in the evening (second mandatory trip). Between two mandatory trips (for example, during lunchtime), EV drivers have a chance for a V2G or G2V trip (an optional trip), so they can declare it in their daily plan submitted to the scheduling entity. This paper assumes that each EV can have a maximum of two optional trips between mandatory trips. As shown in Fig. 3, the first mandatory trip of 88.3% of EVs is randomly scheduled between 06:00 to 10:00. The first optional trip of 93.5% of EVs is randomly planned between 11:00 to 15:00. The second optional trip of 88.8% of EVs is assumed to occur between 13:00 to 18:00. Finally, the second mandatory trip of 89.7% of EVs is supposed to take place between 16:00 to 20:00. Before solving the scheduling problem, the shortest driving routes between the origin of EV e, the location of CS i, and the destination of EV e for each trip are determined by using ArcGIS®. For each hour, the longitude and latitude of each CS, origin and destination of each EV for each trip in a part of San Francisco are used in ArcGIS® to determine the shortest route. Then, the driving distance regarding the routes is used to determine the required energy to travel on each route.

The ambiguity sets for PV generation and wholesale electricity prices are constructed from historical data. We calculated the mean value of PV generation ($\widetilde{Y}_{t,i}^{PV}$) as well as the covariance matrix of PV generation ($\xi_{t,i}$ and $\widehat{\xi}_{t,i}$) in each hour from 100 days data that was obtained from Renewables.ninja for the same area in San Francisco [34]. In addition, for calculating the mean value ($\widetilde{\rho}_t^{\text{WM}}$) and covariance (κ_t) of the wholesale electricity prices, 100 days' worth of prices are used from California ISO [35]. To obtain the prices offered to CSs by the retailers, the day-ahead electricity prices of the wholesale market are multiplied by 4.5 homogeneously to add network maintenance costs, ancillarly services costs, taxes etc. The profit margin of the retailers ($\underline{\alpha}$ and $\overline{\alpha}$) is assumed to be between 5% to 50% in the G2V operation, while the CSs seek

profit in the range of 10% to 30% of the true energy prices. Furthermore, electricity prices offered by CSs are between 60% to 85% less than the prices offered by the retailers during V2G services. The electricity prices sold to the aggregator by CSs are 10% more than what CSs offered to EV drivers for V2G service. The DRCC problems are solved using the Gurobi® solver in Python on a laptop with an Intel Core i7 CPU with a 1.80 GHz processor and 8 GB of RAM.

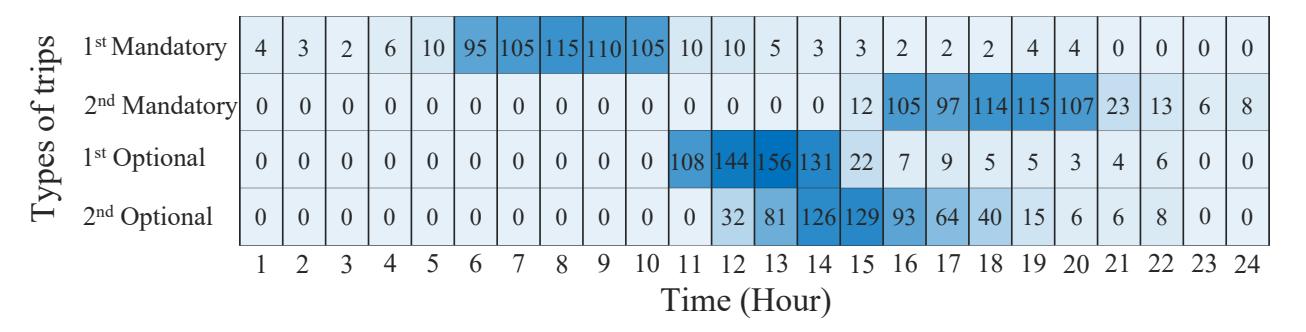


Figure 3: Number of EVs in different mandatory and optional trips; simulation parameters

4.1. Evaluation of Low- to High-Risk Cases

First, we solved the DRCC problem in different layers for different confidence levels ($\nu = 1 - \epsilon$) to investigate the changes in the cost and profits of the stakeholders. For the low-risk (conservative) case studies, the confidence level is high, and the constraints in Eqs. (3d), (3e), (3j), and (3k) in the EV layer, and Eqs. (4b), (4d), and (4e) in the CS layer will be satisfied 95% of the time or more. In the same case study, Eq. (7k) in the retailer layer will be considered with a probability higher than or equal to 90% because the DRCC model will be infeasible at 95% confidence level. It means that the retailers cannot supply CSs under the most conservative condition of the entire ecosystem. It shows the importance of the proposed sequential framework to capture the impact of different layers on each other.

The total net cost of EVs and the total net revenue of CSs and retailers are illustrated in Fig. 5 for different confidence levels. By increasing the confidence level from 0.5 (high-risk case study) to 0.95 (low-risk case study), the total net cost of EVs increased from \$231 to \$803 while the total net revenue of CSs and retailers decreased from \$678 and \$852 to \$498 and \$762, respectively. The reason is that at the lower confidence levels, constraints are relaxed for all stakeholders; hence more options to choose the most optimal V2G and G2V operation. As a result, the risk of not meeting the day-ahead commitment for all stakeholders is much higher in this case in the real-time operation. However, the feasible solution space is much smaller for all stakeholders at higher confidence levels. This way, they pay a premium for higher confidence (lower risks) at the time of delivery of services. Since the DRCC problems for the three layers are solved iteratively, the impact of the conservative operation of one layer leads other players to behave more conservatively. The optimization algorithms convergence rate is shown in Figure 4 for EV and CS layers at 0.95 confidence level, and the retailer layer at 0.9 confidence level. The optimal results are obtained after 23 iterations of the outer loop. Also, we observed that the confidence level affects the optimization runtime. The lower the confidence

level, the higher the computation time because a larger solution space requires more plane cuts to achieve high-quality solutions. For example, it takes 452 minutes to solve the scheduling of the entire ecosystem at a 0.5 confidence level. In comparison, we only needed 47 minutes to solve the problem at a 0.9 confidence level.

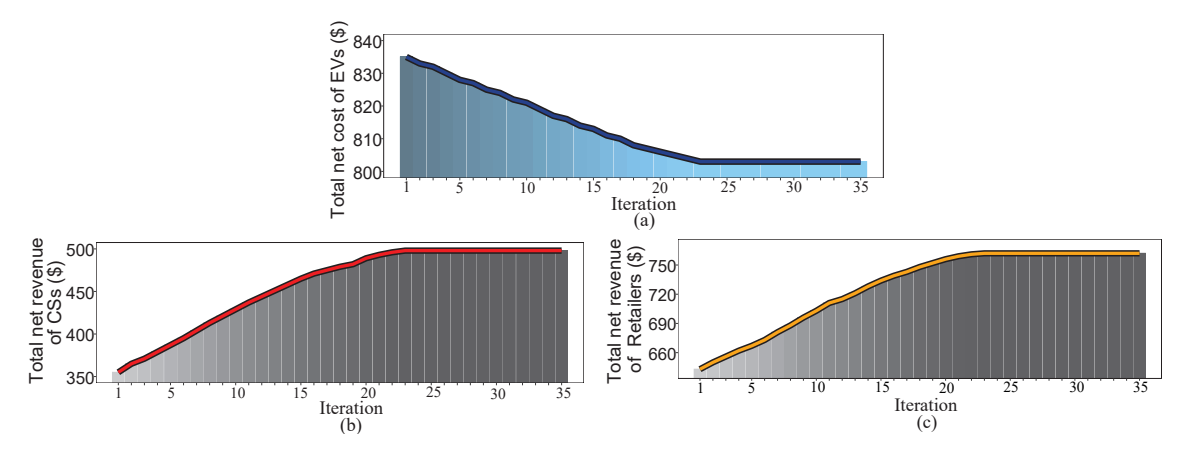


Figure 4: (a) EV layer, (b) CS layer, and (c) Retailer layer objective function values at different iterations for EV and CS layers in 0.95 confidence level and retailer layer in 0.9 confidence level.

The number of EVs scheduled for G2V and V2G operations in each trip is shown in Fig. 6 for 0.95 confidence level in the EV and CS layers and 0.9 at the retailer level. A comparison between Fig. 3 and Fig. 6 shows that most EVs participated in V2G and G2V operation in each type of trip during higher availability hours. For example, the first mandatory trip of 88.3% of the EVs takes place between 06:00 to 10:00, which is similar to the number of EVs that participated in V2G and G2V operation in their first trips (Fig. 6). This is true for the second mandatory trip and the first and second optional trips.

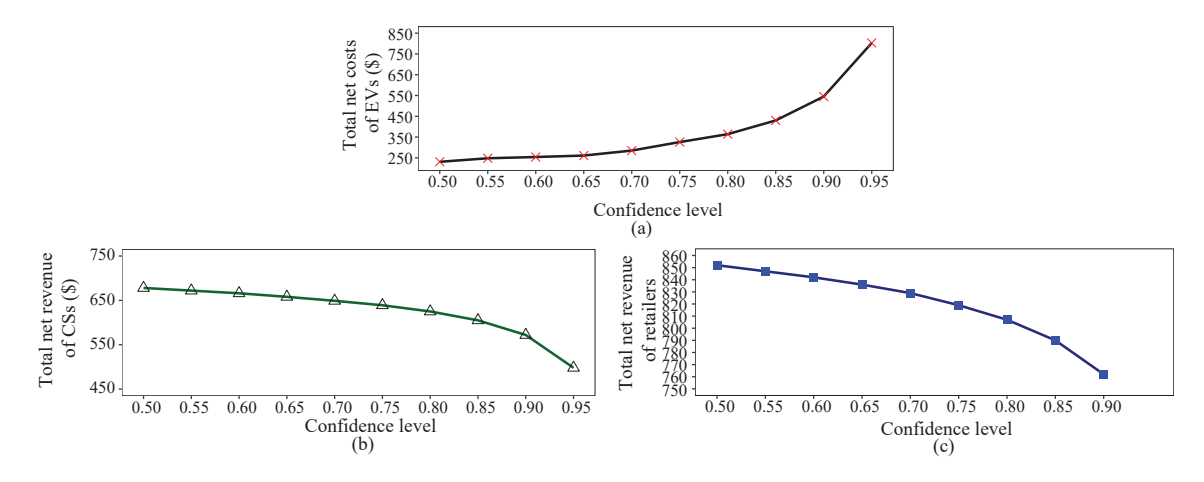


Figure 5: (a) Total net cost of EVs, (b) total net revenue of CSs, and (c) total net revenue of retailers for different confidence levels from 0.5 (high-risk case) to 0.95 (low-risk case)

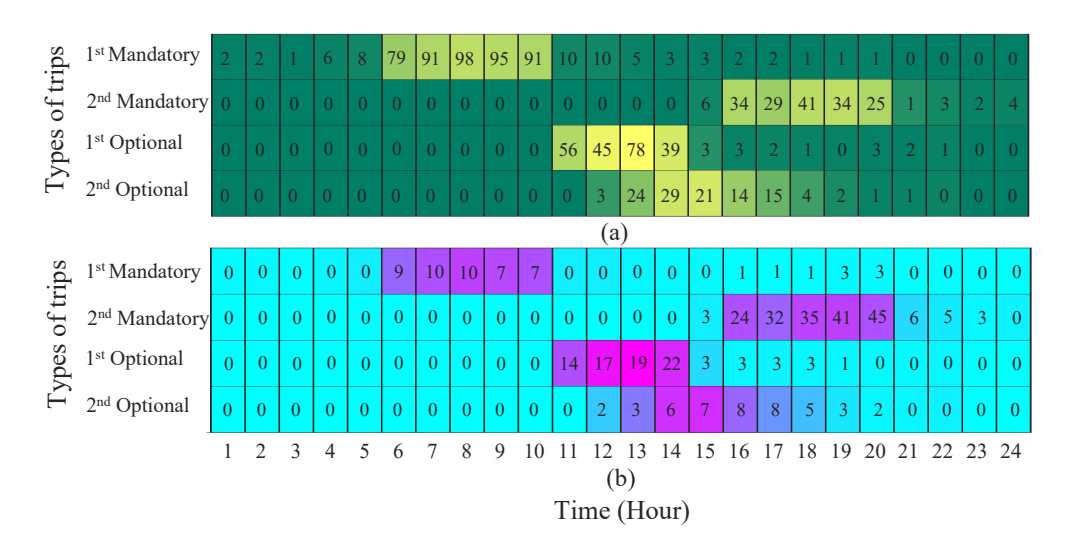


Figure 6: Number of EVs scheduled for (a) G2V and (b) V2G operation

4.2. Validation of DRCC Formulation

In this subsection, the quality of the proposed three-layer joint DRCC framework and the solutions are investigated. The DRCC solutions are valid while the actual confidence level ($\nu_{ac} = 1 - \epsilon_{ac}$) is more than or equal to the theoretical confidence level ($\nu_{th} = 1 - \epsilon_{th}$), which imposed on the formulation and associated simulation of the CC programming. For this investigation, as shown in Fig. 7(a), firstly, we need to consider a theoretical confidence level, ν_{th} , to solve the DRCC problems at different layers iteratively based on the mean value and covariance of stochastic parameters.

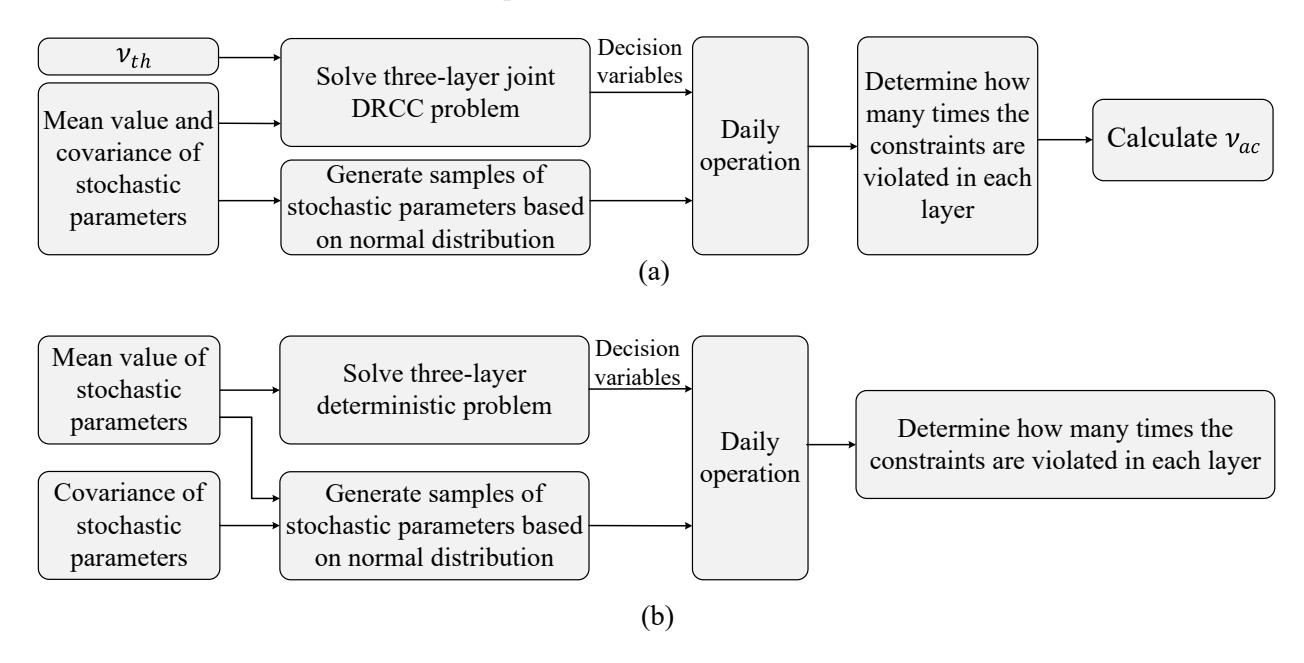


Figure 7: Flowchart of determining actual confidence level in (a) the DRCC problem and (b) the deterministic problem

Afterwards, the optimal solutions jointly used with the samples created for the stochastic parameters

based on normal distribution functions, mean value and covariance of the stochastic parameters (representing the realised value of the parameters in real-time operation) to run a daily operation of the ecosystem. Then, the values obtained from daily operation (e.g., charging and discharging power of EV e at the charging station i at time t and binary variables for the charging station i for charging/discharging EV e at time t) are used in the CCs (Eqs. (3d), (3e), (3j), and (3k) in the EV layer, Eqs. (4b), (4d), and (4e) in the CS layer, and Eq. (7k) in the retailer layer) to investigate how many times the constraints are violated in each layer and obtain the actual confidence level, ν_{ac} . This process is repeated for different values of theoretical confidence level in each layer, i.e., $\nu_{th} \in [0.5, 0.9]$, to obtain the mean values of the actual confidence level, ν_{ac} . While we used normal distribution in this part of our simulation study, it should be noted that the reformulation of the single-sided and double-sided CCs, presented in Appendix A, is independent of the type of probability distribution function. Also, we calculated the CCs violations in a deterministic day-ahead scheduling framework using the process shown in Fig. 7(b) for comparison.

The actual confidence levels obtained by the proposed stochastic framework are illustrated in Fig. 8 for each layer compared to the theoretical ones. Please note that for determining the actual confidence level of each layer, the theoretical confidence level of other layers is kept constant at 0.9. It can be seen from the figure that the actual confidence level is always higher than the theoretical one. In addition, Fig. 8 shows that the DRCC programming is more conservative on the lower range of theoretical confidence levels. The simulation results for the deterministic scheduling framework show the actual confidence levels of 0.71, 0.79, and 0.75 for the EV, CS, and retailer layers, respectively, which are lower than the lowest actual confidence level of the proposed stochastic framework.

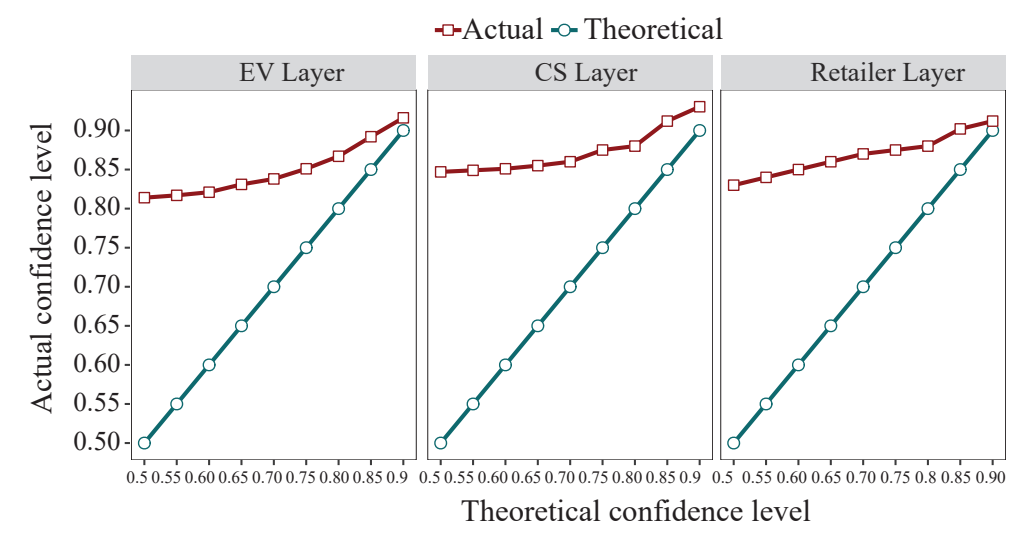


Figure 8: DRCC validation for EV, CS, and Retailer layers

In addition, the number of unique EVs that violated the CCs (Eqs. (3d), (3e), (3j), and (3k)) in the proposed DRCC framework are shown for different confidence levels in Fig. 9. As expected, the number of unique EVs with constraint violation decreased by increasing the confidence level in the EV layer. Further-

more, the number of unique EVs that do not reach their destination (due to lower SOC limit violation) are shown in Fig. 10 for different confidence levels, which decreases by increasing the confidence level. It shows the importance of the proposed framework in reducing EV drivers' frustration, which contributes to lowering range anxiety. In addition, 272 unique EVs could not reach their destination in the deterministic problem, which is more than the one obtained at the lowest confidence level, 0.5, in the proposed DRCC framework.

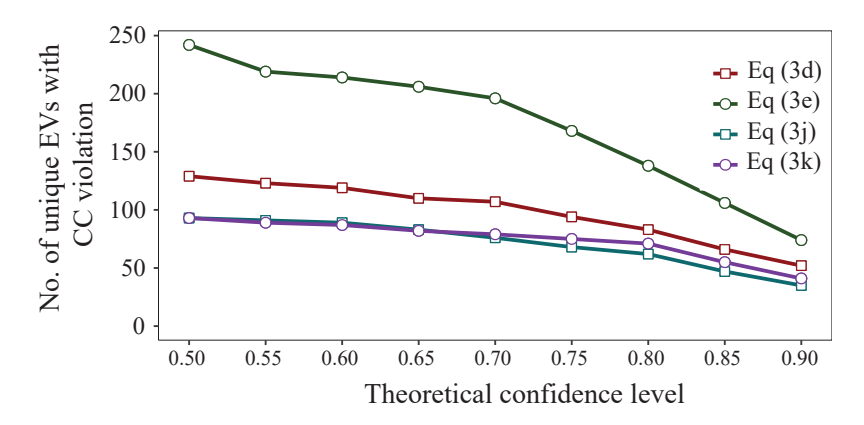


Figure 9: Number of unique EVs violating their CCs at least once a day at different confidence levels in the EV layer in the proposed DRCC framework.

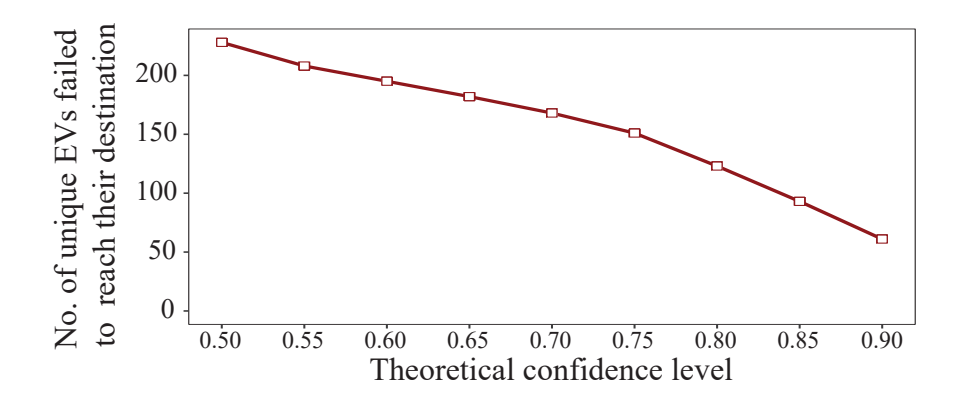


Figure 10: Number of unique EVs which does not fulfil their mandatory trips in the proposed DRCC framework at different confidence level.

4.3. Impact of Temporal Correlation of PV Generation

This section investigates the impact of considering the temporal correlation of PV generation in CSs. First, we calculated the root mean square error (RMSE) of PV generation with and without considering the temporal correlation in Eq. (4e) for all CSs. The simulation results show that the RMSE has improved from 17.8% to 16.3% by considering PV temporal correlations. In addition, we calculated the additional number of unique EVs that could not fulfil their mandatory trips due to violating lower SOC limit at different confidence levels after removing the PV correlation effect in the CS layer, shown in Fig. 11. Two more EVs won't reach their destination at a 0.95 confidence level if we don't consider the PV correlation. By decreasing the confidence level in the CS layer from 0.95 to 0.5 in the absence of PV correlation, the number

of additional EVs that couldn't fulfil their mandatory trips increased to nine. It clearly shows the impact of PV temporal correlation on the successful scheduling of the ecosystem.

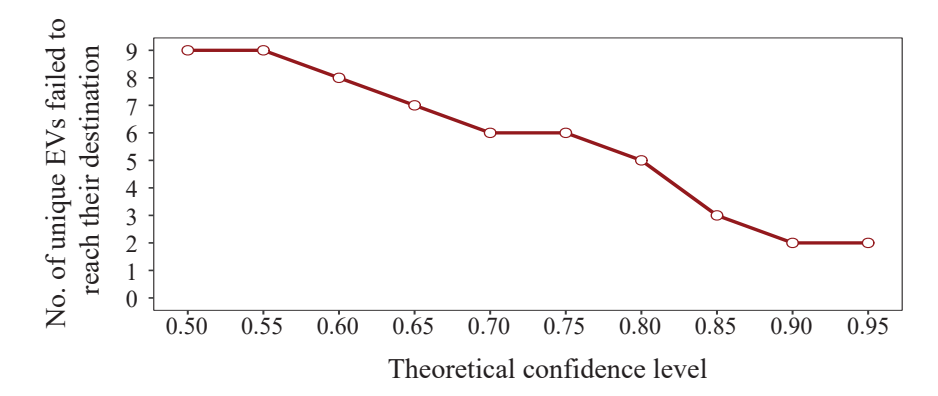


Figure 11: Additional number of unique EVs that could not reach their destination without PV correlation constraint at the CS layer.

4.4. The Impact of Three-Layer Joint DRCC Problem

Table 1 shows a comparison between the cost/revenue of three stakeholders for two different cases as defined below:

- Case I: This is the case in which the proposed three-layer DRCC optimisation problem is solved iteratively to find the solution considering the mutual impacts of the stochastic behaviour of the stakeholders in an uncertain environment. Please note that this is the proposed approach in this paper.
- Case II: The DRCC optimisation problems in the three layers are solved individually, not iteratively.
 Thus, the mutual impacts of the stochastic behaviour of the stakeholders in an uncertain environment are not considered.

Similar mandatory and optional trips and EV drivers' preferences are considered in both case studies. The optimal cost of EVs at a 0.95 confidence level and optimal revenue for CS and retailer layers at 0.95 and 0.9 confidence levels, respectively, for both cases, can be observed in Table 1. The total net cost of EVs in Case II increased by 2.6% and the total net revenue of CSs and retailers decreased by 4.0% and 1.8%, respectively, compared to Case I. This study shows the effectiveness of the proposed iterative method by considering the impact of uncertainty of a stakeholder on the other ones.

5. Conclusion

This paper proposes a three-layer joint DRCC model for the future e-mobility ecosystem including EVs, CSs, and retailers to schedule V2G and G2V services in the day ahead in an uncertain environment with unknown probability distribution functions. The interactions between the stochastic parameters of the three

Table 1: Total net cost and revenue of all stakeholders

Cost/Revenue	Case I	Case II
Total net cost of EVs (\$)	803	824
Total net revenue of CSs (\$)	498	478
Total net revenue of retailers (\$)	762	748

stakeholders are considered in the proposed iterative model to improve the performance of the scheduling system for the entire e-mobility ecosystem. Also, a second-order cone programming reformulation of the DRCC model is implemented to reformulate the double-sided CCs. In addition, the impact of the temporal correlation of uncertain PV generation on the CSs operation is considered. The simulation results show that the choice of confidence level significantly affects the cost and revenue of the stakeholders as well as the accuracy of the schedules in real-time operation. For a low-risk case study, the model estimates a 247.3% increase in the total net cost of EVs compared to a high-risk case study, and a 26.6% and 10.6% decrease in the total net revenue of CSs and retailers, respectively. In addition, the number of unique EVs that failed to reach their destination has decreased from 272 in the deterministic scheduling model to 61 in the low-risk case study. The simulation results prove the necessity of such planning frameworks to reduce the risks for all stakeholders, which in turn facilitates higher adoption of EVs by the end-users and investors. In future studies, we intend to explore different reformulations of DRCC in each layer that is less conservative at lower confidence levels. Also, to make the scheduling problem more flexible for the EV drivers, a new formulation will be developed to automatically select the best time for optional trips within a pre-defined range of time by the EV drivers.

References

- M. K. Daryabari, R. Keypour, H. Golmohamadi, Stochastic energy management of responsive plug-in electric vehicles characterizing parking lot aggregators, Applied Energy 279 (2020) 115751.
- [2] J. Su, T. Lie, R. Zamora, A rolling horizon scheduling of aggregated electric vehicles charging under the electricity exchange market, Applied Energy 275 (2020) 115406.
- [3] J. Zhao, Z. Xu, J. Wang, C. Wang, J. Li, Robust distributed generation investment accommodating electric vehicle charging in a distribution network, IEEE Transactions on Power Systems 33 (5) (2018) 4654–4666.
- [4] A. Hajebrahimi, I. Kamwa, M. M. A. Abdelaziz, A. Moeini, Scenario-wise distributionally robust optimization for collaborative intermittent resources and electric vehicle aggregator bidding strategy, IEEE Transactions on Power Systems 35 (5) (2020) 3706–3718.
- [5] W. Sun, F. Neumann, G. P. Harrison, Robust scheduling of electric vehicle charging in lv distribution networks under uncertainty, IEEE Transactions on Industry Applications 56 (5) (2020) 5785–5795.
- [6] Y. Zhou, D. K. Yau, P. You, P. Cheng, Optimal-cost scheduling of electrical vehicle charging under uncertainty, IEEE Transactions on Smart Grid 9 (5) (2017) 4547–4554.
- [7] O. Fallah-Mehrjardi, M. H. Yaghmaee, A. Leon-Garcia, Charge scheduling of electric vehicles in smart parking-lot under future demands uncertainty, IEEE Transactions on Smart Grid 11 (6) (2020) 4949– 4959.
- [8] E. Roos, D. den Hertog, Reducing conservatism in robust optimization, INFORMS Journal on Computing 32 (4) (2020) 1109–1127.
- [9] L. Jian, Y. Zheng, X. Xiao, C. Chan, Optimal scheduling for vehicle-to-grid operation with stochastic connection of plug-in electric vehicles to smart grid, Applied Energy 146 (2015) 150–161.
- [10] Y. Zheng, H. Yu, Z. Shao, L. Jian, Day-ahead bidding strategy for electric vehicle aggregator enabling multiple agent modes in uncertain electricity markets, Applied Energy 280 (2020) 115977.
- [11] M.-W. Tian, S.-R. Yan, X.-X. Tian, M. Kazemi, S. Nojavan, K. Jermsittiparsert, Risk-involved stochastic scheduling of plug-in electric vehicles aggregator in day-ahead and reserve markets using downside risk constraints method, Sustainable Cities and Society 55 (2020) 102051.
- [12] Z. Wang, P. Jochem, W. Fichtner, A scenario-based stochastic optimization model for charging scheduling of electric vehicles under uncertainties of vehicle availability and charging demand, Journal of Cleaner Production 254 (2020) 119886.

- [13] M. Schücking, P. Jochem, Two-stage stochastic program optimizing the cost of electric vehicles in commercial fleets, Applied Energy 293 (2021) 116649.
- [14] T. Zhang, W. Chen, Z. Han, Z. Cao, Charging scheduling of electric vehicles with local renewable energy under uncertain electric vehicle arrival and grid power price, IEEE Transactions on Vehicular Technology 63 (6) (2013) 2600–2612.
- [15] Y. Wu, J. Zhang, A. Ravey, D. Chrenko, A. Miraoui, Real-time energy management of photovoltaic-assisted electric vehicle charging station by markov decision process, Journal of Power Sources 476 (2020) 228504.
- [16] S. Faridimehr, S. Venkatachalam, R. B. Chinnam, A stochastic programming approach for electric vehicle charging network design, IEEE Transactions on Intelligent Transportation Systems 20 (5) (2018) 1870–1882.
- [17] S. Liu, A. H. Etemadi, A dynamic stochastic optimization for recharging plug-in electric vehicles, IEEE Transactions on Smart Grid 9 (5) (2017) 4154–4161.
- [18] B. Wang, Y. Wang, H. Nazaripouya, C. Qiu, C.-C. Chu, R. Gadh, Predictive scheduling framework for electric vehicles with uncertainties of user behaviors, IEEE Internet of Things Journal 4 (1) (2016) 52–63.
- [19] S. Zeynali, N. Nasiri, M. Marzband, S. N. Ravadanegh, A hybrid robust-stochastic framework for strategic scheduling of integrated wind farm and plug-in hybrid electric vehicle fleets, Applied Energy 300 (2021) 117432.
- [20] B. Zeng, H. Dong, R. Sioshansi, F. Xu, M. Zeng, Bi-level robust optimization of electric vehicle charging stations with distributed energy resources, IEEE Transactions on Industry Applications (2020).
- [21] X. Bai, W. Qiao, Robust optimization for bidirectional dispatch coordination of large-scale v2g, IEEE Transactions on Smart Grid 6 (4) (2015) 1944–1954.
- [22] H. Yang, X. Xie, A. V. Vasilakos, Noncooperative and cooperative optimization of electric vehicle charging under demand uncertainty: A robust stackelberg game, IEEE Transactions on vehicular technology 65 (3) (2015) 1043–1058.
- [23] N. Korolko, Z. Sahinoglu, Robust optimization of ev charging schedules in unregulated electricity markets, IEEE Transactions on Smart Grid 8 (1) (2015) 149–157.
- [24] Y. Cao, L. Huang, Y. Li, K. Jermsittiparsert, H. Ahmadi-Nezamabad, S. Nojavan, Optimal scheduling of electric vehicles aggregator under market price uncertainty using robust optimization technique, International Journal of Electrical Power & Energy Systems 117 (2020) 105628.

- [25] Y. Cui, Z. Hu, H. Luo, Optimal day-ahead charging and frequency reserve scheduling of electric vehicles considering the regulation signal uncertainty, IEEE Transactions on Industry Applications 56 (5) (2020) 5824–5835.
- [26] Z. Liu, Q. Wu, S. S. Oren, S. Huang, R. Li, L. Cheng, Distribution locational marginal pricing for optimal electric vehicle charging through chance constrained mixed-integer programming, IEEE Transactions on Smart Grid 9 (2) (2016) 644–654.
- [27] H. Liu, Y. Zhang, S. Ge, C. Gu, F. Li, Day-ahead scheduling for an electric vehicle pv-based battery swapping station considering the dual uncertainties, IEEE Access 7 (2019) 115625–115636.
- [28] B. Wang, P. Dehghanian, D. Zhao, Chance-constrained energy management system for power grids with high proliferation of renewables and electric vehicles, IEEE Transactions on Smart Grid 11 (3) (2019) 2324–2336.
- [29] F. Pourahmadi, J. Kazempour, C. Ordoudis, P. Pinson, S. H. Hosseini, Distributionally robust chance-constrained generation expansion planning, IEEE Transactions on Power Systems 35 (4) (2019) 2888–2903.
- [30] M. B. Tookanlou, S. A. Pourmousavi, M. Marzband, An optimal day-ahead scheduling framework for e-mobility ecosystem operation with drivers preferences, IEEE Transactions on Power Systems (2021).
- [31] G. A. Hanasusanto, D. Kuhn, Conic programming reformulations of two-stage distributionally robust linear programs over wasserstein balls, Operations Research 66 (3) (2018) 849–869.
- [32] P. M. Esfahani, D. Kuhn, Data-driven distributionally robust optimization using the wasserstein metric: Performance guarantees and tractable reformulations, Mathematical Programming 171 (1) (2018) 115–166.
- [33] W. Xie, S. Ahmed, Distributionally robust chance constrained optimal power flow with renewables: A conic reformulation, IEEE Transactions on Power Systems 33 (2) (2017) 1860–1867.
- [34] Renewables.ninja for san francisco, available at: https://www.renewables.ninja/(2019).
- [35] California ISO, available at: http://www.oasis.caiso.com (2019).

Appendix A. Reformulation of single-sided and double-sided chance constraints

As mentioned before, we aim to reformulate the single-sided and double-sided chance constraints (CCs) of EV, CS, and retailer layer based on the two *Theorems* developed in [33].

Theorem 1. Suppose the ambiguity set defined as Ξ in Eq. (2) in the original manuscript, then the equivalents of single-sided chance constraints in Eqs. (A.1a) and (A.1b) are as Eqs. (A.2a) and (A.2b), respectively.

$$\inf_{\mathbb{D}_{\epsilon} \Xi} \mathbb{P}\left[a(x)^T \Omega + b(x) \le L\right] \ge 1 - \epsilon, \tag{A.1a}$$

$$\inf_{\mathbb{P}_{\epsilon} \Xi} \mathbb{P} \left[a(x)^T \Omega + b(x) \ge -L \right] \ge 1 - \epsilon, \tag{A.1b}$$

$$b(x) + \sqrt{\frac{1 - \epsilon}{\epsilon}} \sqrt{a(x)^T \Sigma a(x)} \le L,$$
(A.2a)

$$-b(x) + \sqrt{\frac{1-\epsilon}{\epsilon}} \sqrt{a(x)^T \Sigma a(x)} \le L,$$
(A.2b)

where a(x) and b(x) are affine mappings, and Ω is a random variable with zero mean and covariance matrix, Σ .

Theorem 2. Suppose the ambiguity set defined as Ξ in Eq. (2) of the original manuscript, then the equivalent of a double-sided chance constraint in Eq. (A.3) can be reformulated as in Eqs. (A.4) with two additional variables $(y \text{ and } \pi)$.

$$\inf_{\mathbb{P} \in \Xi} \mathbb{P}[|a(x)^T \Omega + b(x)| \le L] \ge 1 - \epsilon. \tag{A.3}$$

$$\left\{
\begin{aligned}
y^2 + a(x)^T \Sigma a(x) &\le \epsilon (L - \pi)^2, \\
|b(x)| &\le y + \pi, \\
L &\ge \pi \ge 0, y \ge 0
\end{aligned}
\right\}.$$
(A.4)

Appendix A.1. Reformulation of Chance Constraints of EV layer

According to reformulation of single-sided and double-sided chance constraints explained in Eqs. (A.1a)(A.4), the reformulation of the constraints in Eq. (3d) in the original manuscript will be as of Eqs. (A.5a),
(A.5b), and (A.5c). For example, in Eq. (3d), we let $a(x) = \mathbf{1}^T$, $b(x) = \widetilde{SOC}_e + A_{t,e,i} - \sum_{t=1}^t \frac{\zeta_{t,e} \cdot \gamma_e}{\overline{E}_e} \cdot (1 - \Gamma_{t,e,i} - \Pi_{t,e,i}) - \frac{\overline{C_{t,e,i} \cdot \gamma_e}}{\overline{E}_e} \cdot (\Gamma_{t,e,i} + \Pi_{t,e,i}) - \frac{\overline{SOC}_e + SOC_e}{2}$, and $L = \frac{\overline{SOC}_e - SOC_e}{2}$. In addition, we convert Eq. (3e) in the original manuscript to Eqs. (A.5d), (A.5e), and (A.5f), as well as Eq. (3j) and (3k) in the original manuscript to (A.5g), and (A.5h), respectively.

$$q_{t,e,i}^2 + 1^T \Sigma_e 1 \le \epsilon_{th}^{EV} \left(\frac{\overline{SOC}_e - \underline{SOC}_e}{2} - I_{t,e,i} \right)^2, \tag{A.5a}$$

$$\left| \overline{SOC}_{e} + A_{t,e,i} - \sum_{t=1}^{t} \frac{\zeta_{t,e} \cdot \gamma_{e}}{\overline{E}_{e}} \cdot (1 - \Gamma_{t,e,i} - \Pi_{t,e,i}) - \frac{\mathcal{O}_{t,e,i} \cdot \gamma_{e}}{\overline{E}_{e}} \cdot (\Gamma_{t,e,i} + \Pi_{t,e,i}) - \frac{\overline{SOC}_{e} + \underline{SOC}_{e}}{2} \right|$$
(A.5b)

 $\leq q_{t,e,i} + I_{t,e,i}$

$$\frac{\overline{SOC}_e - \underline{SOC}_e}{2} \ge I_{t,e,i} \ge 0, \quad q_{t,e,i} \ge 0, \tag{A.5c}$$

$$q_{T,e,i}^2 + 1^T \Sigma_e 1 \le \epsilon_{th}^{EV} \left(\frac{\overline{SOC}_e - SOC_e^{end}}{2} - I_{T,e,i} \right)^2, \tag{A.5d}$$

$$\left| \widetilde{SOC}_{e} + A_{T,e,i} - \sum_{t=1}^{T} \frac{\zeta_{t,e} \cdot \gamma_{e}}{\overline{E}_{e}} \cdot (1 - \Gamma_{t,e,i} - \Pi_{t,e,i}) - \frac{\mathcal{O}_{T,e,i} \cdot \gamma_{e}}{\overline{E}_{e}} \cdot (\Gamma_{T,e,i} + \Pi_{T,e,i}) - \frac{SOC_{e}^{end} + \underline{SOC}_{e}}{2} \right|$$
(A.5e)

 $\leq q_{T,e,i} + I_{T,e,i}$

$$\frac{\overline{SOC}_e - SOC_e^{end}}{2} \ge I_{T,e,i} \ge 0, \quad q_{T,e,i} \ge 0, \tag{A.5f}$$

$$\rho_{t,i}^{+}.X_{t,e,i}^{+} - \vartheta_{e} \cdot \Gamma_{t,e,i} - \widehat{\rho}_{t,i}^{+} \cdot \overline{E}_{e} \cdot \Gamma_{t,e,i} \cdot \left(\widehat{SOC}_{e} + \widehat{A}_{t,e,i}, \right) \\
- \frac{\widehat{\mathcal{O}}_{t,e,i}.\gamma_{e}}{\overline{E}_{e}} + \widehat{\rho}_{t,i}^{+} \cdot \overline{E}_{e} \cdot (1 - \Gamma_{t,e,i}) \cdot \sum_{t=1}^{t} \frac{\zeta_{t,e} \cdot \gamma_{e}}{\overline{E}_{e}} \\
+ \sqrt{\frac{1 - \epsilon_{th}^{EV}}{\epsilon_{th}^{EV}} \cdot \Sigma_{e}} \cdot \mathbf{1}^{T} \cdot \overline{E}_{e} \cdot \Gamma_{t,e,i} \cdot \widehat{\rho}_{t,i}^{+} \leq 0, \\
- \widehat{\rho}_{t,i}^{-}.X_{t,e,i}^{-} + \mathcal{G}_{e}.\Pi_{t,e,i} + \widehat{\rho}_{t,i}.\overline{E}_{e}.\Pi_{t,e,i}. \left(\widehat{SOC}_{e} + \widehat{A}_{t,e,i} \right) \\
- \frac{\widehat{\mathcal{O}}_{t,e,i}.\gamma_{e}}{\overline{E}_{e}} - \widehat{\rho}_{t,i}.\overline{E}_{e}.(1 - \Pi_{t,e,i}) \cdot \sum_{t=1}^{t} \frac{\zeta_{t,e}.\gamma_{e}}{\overline{E}_{e}} \\
+ \sqrt{\frac{1 - \epsilon_{th}^{EV}}{\epsilon_{th}^{EV}} \cdot \Sigma_{e}} \cdot \mathbf{1}^{T}.\overline{E}_{e}.\Pi_{t,e,i}.\widehat{\rho}_{t,i} \leq 0. \tag{A.5h}$$

Appendix A.2. Reformulation of chance constraints of CS layer

Using *Theorem 1*, Eq. (4b) in the original manuscript is reformulated as Eq. (A.6a). Also, Eqs. (4d) and (4e) in the original manuscript are converted to Eqs. (A.6b)-(A.6d) and Eqs. (A.6e)-(A.6g), respectively, based on *Theorem 2*.

$$-\widetilde{Y}_{t,i}^{\text{PV}} - Y_{t,i}^{GU} - Y_{t,i,r}^{re} - Y_{t,i}^{-} - \sum_{e \in E} X_{t,e,i}^{-} + \frac{\sum_{e \in E} X_{t,e,i}^{-}}{\eta_{i}^{\text{CH}}} + \frac{\sum_{e \in E} X_{t,e,i}^{+}}{\eta_{i}^{\text{CH}}} + Y_{t,i}^{+} + \sqrt{\frac{1 - \epsilon_{th}^{CS}}{\epsilon_{th}^{CS}} \cdot \Sigma_{t,i}^{PV}} + \leq \varepsilon$$

$$\forall t \in T, \forall i \in S, \forall r \in R,$$
(A.6a)

$$z_{t,i}^2 + \mathbf{1}^T \cdot \Sigma_{t,i}^{PV} \cdot \mathbf{1} \le \epsilon_{th}^{CS} \left(\frac{\overline{E}_i^{PV}}{2} - \mu_{t,i} \right)^2, \tag{A.6b}$$

$$\left| \widetilde{Y}_{t,i}^{PV} - \frac{\overline{E}_{i}^{PV}}{2} \right| \le z_{t,i} + \mu_{t,i}, \tag{A.6c}$$

$$\frac{\overline{E}_i^{PV}}{2} \ge \mu_{t,i} \ge 0, \quad z_{t,i} \ge 0, \tag{A.6d}$$

$$U_{t,i} - \mathbf{1}^T \widehat{\Sigma}_{t,i} \mathbf{1} \le \epsilon_{th}^{CS} \left(\frac{\overline{r}_i^{PV} - \underline{r}_i^{PV}}{2} - V_{t,i} \right)^2, \tag{A.6e}$$

$$\left| \widetilde{Y}_{t,i}^{PV} - \widetilde{Y}_{(t-1),i}^{PV} - \frac{\underline{r}_{i}^{PV} + \overline{r}_{i}^{PV}}{2} \right| \le U_{t,i} + V_{t,i}, \tag{A.6f}$$

$$\frac{\overline{r}_{i}^{PV} - \underline{r}_{i}^{PV}}{2} \ge V_{t,i} \ge 0, \quad U_{t,i} \ge 0,$$
(A.6g)

Appendix A.3. Reformulation of chance constraints of retailer layer

Based on **Theorem 2**, the double-sided CC in Eq. (7k) in the original manuscript is reformulated as Eqs. (A.7a)-(A.7c)

$$x_{t,r}^2 + \frac{1}{\widetilde{\rho}_t^{\text{WM}}} \cdot \tau_t \le \epsilon_{th}^{re} \left(\frac{\overline{\alpha}_t - \underline{\alpha}_t}{2} - l_{t,r} \right)^2, \tag{A.7a}$$

$$\left| \frac{\rho_{t,r}^{re}}{\widetilde{\rho}_t^{\text{WM}}} - \frac{\overline{\alpha}_t + \underline{\alpha}_t}{2} \right| \le x_{t,r} + l_{t,r}, \tag{A.7b}$$

$$0 \le l_{t,r} \le \frac{\overline{\alpha}_t - \underline{\alpha}_t}{2}, \quad x_{t,r} \ge 0. \tag{A.7c}$$